



1 **Does size matter? Pico-phytoplankton cell size affects biomass distribution and nutrient**  
2 **limitation in the oligotrophic Eastern Mediterranean Sea**

3 Elad Albagly<sup>1,2</sup> and Eyal Rahav<sup>1,3,4</sup>

4 <sup>1</sup> Israel Oceanographic and Limnological Research, Haifa, Israel.

5 <sup>2</sup> Koret School of Veterinary Medicine, The Hebrew University of Jerusalem, Rehovot, Israel.

6 <sup>3</sup> Institute of Marine Science, University of California, Santa Cruz, CA, USA.

7 <sup>4</sup> Department of Earth and Environmental Science, Ben-Gurion University of the Negev, Beer  
8 Sheva, Israel.

9

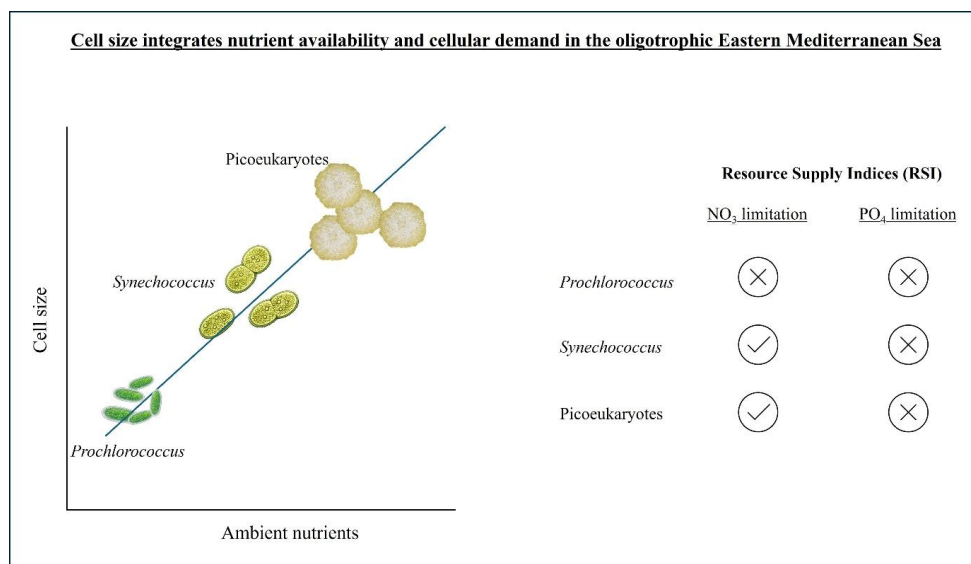
10 **Correspondence:** E. Rahav ([eyal.rahav@ocean.org.il](mailto:eyal.rahav@ocean.org.il); [eyrahav@ucsc.edu](mailto:eyrahav@ucsc.edu))

11

12 **Abstract.** The Eastern Mediterranean Sea (EMS) is one of the most oligotrophic marine  
13 environments in the world, characterized by extreme nutrient scarcity and strong water-column  
14 stratification. In such systems, pico-phytoplankton typically dominate primary production, yet  
15 how cell size structures biomass distribution and nutrient limitation remains poorly  
16 constrained. Here, we examined the spatial and vertical variability of pico-phytoplankton cell  
17 size, abundance, and nutrient status in the easternmost Mediterranean Sea during oligotrophic  
18 summer stratification. Using flow cytometry and microscopy, we quantified the cell volumes  
19 of *Prochlorococcus*, *Synechococcus*, and pico-eukaryotes and combined these with ambient  
20 nutrient concentrations to estimate cellular nutrient quotas and Resource Supply Indices (RSI).  
21 All three groups exhibited increasing cell size with depth and from offshore to coastal waters,  
22 coinciding with higher nutrient availability and chlorophyll concentrations. *Synechococcus* and  
23 pico-eukaryotes were consistently larger in coastal and deeper waters, whereas  
24 *Prochlorococcus* maintained small and relatively constant cell size across environments. RSI  
25 analysis revealed widespread nitrogen limitation for *Synechococcus* and pico-eukaryotes  
26 ( $RSI_n < 1$ ), while phosphorus was generally sufficient ( $RSI_p > 1$ ). In contrast, *Prochlorococcus*  
27 remained largely unconstrained by either nitrogen or phosphorus, reflecting its low cellular  
28 nutrient demand and streamlined physiology. These results demonstrate that cell size is a  
29 powerful integrator of environmental forcing and ecological strategy in oligotrophic seas. The  
30 dominance of small *Prochlorococcus* cells under extreme nutrient scarcity imply how stable  
31 ocean stratification and nutrient decline may reshape microbial communities and  
32 biogeochemical cycling in the future oligotrophic oceans.



### 33 Graphical abstract



34

35 **Keywords:** Pico-phytoplankton; Eastern Mediterranean Sea, Resource Supply Indices,  
36 Oligotrophy; Cell-size

37

### 38 1 Introduction

39 Cell size is a foundational functional trait that shapes phytoplankton physiology, population  
40 dynamics, and community structure (Chisholm, 1992; Finkel et al., 2010; Litchman and  
41 Klausmeier, 2008). Across taxa, phytoplankton cell volume spans several orders of magnitude.  
42 Generally, in low-productivity oligotrophic water, pico-phytoplankton cells (<2-3 μm in  
43 diameter) dominate the autotrophic community (Reich et al., 2022; Yacobi et al., 1995). Pico-  
44 phytoplankton are small-sized phytoplankton that are composed of both prokaryotes and  
45 eukaryotes. They hold a pivotal role in the global primary production (some estimates suggest  
46 they contribute ~50% of the global rates, e.g., Field et al., 1998; Huang et al., 2021), making  
47 them a highly ecological-important group that affect the 'biological pump' and carbon  
48 sequestration in the deep oceans (Falkowski, 1997), and thus play an important role in  
49 regulating the global carbon cycle (Beardall et al., 2017; Chisholm, 2000).

50 Pico-eukaryotes are a taxonomically diverse group and include several algal phyla (Vaulot et  
51 al., 2008), while the prokaryotes belong to the phylum cyanobacteria are subdivided into the  
52 genera *Prochlorococcus* and *Synechococcus*, with each group having many ecotypes that



53 dominate in different ocean regions (e.g., high-light vs. low-light adapted, Flombaum et al.,  
54 2013). Pico-phytoplankton often dominate the phytoplankton biomass under oligotrophic  
55 conditions such as in the subtropical gyres (Alvain et al., 2005), the northern Red Sea (Lindell  
56 and Post, 1995; Reich et al., 2024), and the Eastern Mediterranean Sea (Rahav and Berman-  
57 Frank, 2023). In contrast, productive waters are typically dominated by larger micro-  
58 phytoplankton such as diatoms and dinoflagellates ( $>20\ \mu\text{m}$ ) and exhibit simpler trophic  
59 pathways and higher particle sinking rates (Chkili et al., 2023). Under these conditions, the  
60 efficiency of the “biological pump” is greater than in oligotrophic systems, either directly via  
61 the sinking of ungrazed large cells or indirectly through aggregated particles and zooplankton  
62 fecal pellets (also referred to as “marine snow”) (Boyd and Trull, 2007; Guidi et al., 2009).

63 Phytoplankton cellular composition, metabolic activity, nutrient uptake kinetics, and growth  
64 rate often exhibit pronounced cell-size dependence (Chisholm, 1992; Kiørboe, 1993; Marañón,  
65 2015). Generally, as cells become larger, nutrient supply per unit volume theoretically declines  
66 (Kiørboe, 1993; Raven, 1998), raising the nutrient concentration threshold required to sustain  
67 a given growth rate (Chisholm, 1992). These biophysical constraints confer a clear advantage  
68 to small pico-phytoplankton cells due to their high-surface-to-volume ratio, which potentially  
69 makes them excellent competitors for nutrient acquisition from their surrounding in  
70 oligotrophic environments (Raven, 1998). Experimental studies consistently support an  
71 allometric pattern in which cell size is inversely related to growth rate and biomass-specific  
72 metabolic rate (Banse, 1982; Geider et al., 1986; Sommer, 1989). A key limitation of much of  
73 this literature, however, is taxonomic and size bias: most analyses have focused on large-size  
74 species, thereby excluding pico-phytoplankton (Marañón, 2015).

75 The variability of nutrients, pico-phytoplankton abundance/biomass, and primary production  
76 in the EMS have been investigated previously (e.g., Belkin et al., 2022; Raveh et al., 2015;  
77 Yacobi et al., 1995). These studies (and others) generally showed that pico-phytoplankton cells  
78 predominate phytoplankton biomass in the EMS (Rahav and Berman-Frank, 2023; Yacobi et  
79 al., 1995), and that the variability in pico-phytoplankton standing stocks and primary  
80 production are often related to depth within the photic water column (Yogev et al., 2011),  
81 circulation patterns (e.g., cyclonic/anti-cyclonic eddies, Belkin et al., 2022; Rahav et al., 2013),  
82 and to a lesser extent seasonality (Reich et al., 2022). Although the EMS is considered as one  
83 of the most oligotrophic seas in the world (Krom et al., 2013), and a natural laboratory to  
84 investigate ocean warming and climate changes (Ben-Ezra et al., 2021), it has received little  
85 attention compared to other oligotrophic regimes, particularly in terms of phytoplankton cell  
86 sizes and how it affects community metabolism. Thus, investigating pico-phytoplankton size



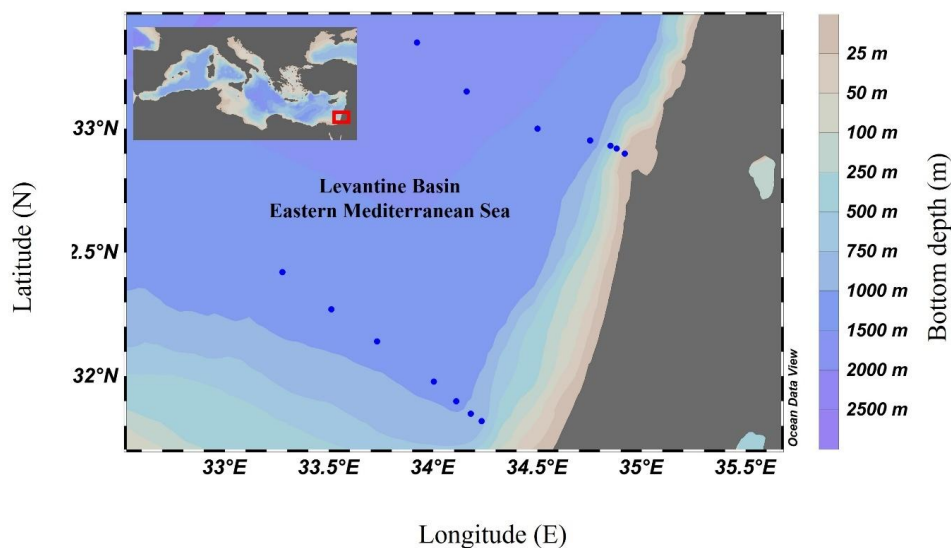
87 distribution and biomass in respect to key environmental factors (e.g., nutrients) is critical to  
88 understand their contributions to carbon cycles and sequestration in the oligotrophic oceans.  
89 Here, we investigated the spatial and vertical distribution of pico-phytoplankton and their size  
90 across the photic layer of Israel's Exclusive Economic Zone (EEZ), in the EMS. We show that  
91 pico-phytoplankton biomass and size generally increase with depth, and from the coast to the  
92 offshore water, coinciding inorganic nutrients availability. Additional calculations based on  
93 ambient nutrient concentrations and cell size of different pico-phytoplankton groups reveal that  
94 *Synechococcus* and pico-eukaryotes are primarily N limited, while *Prochlorococcus* are not N  
95 nor P limited based on this matrix, suggesting other controls of this cyanobacterial genus in the  
96 EMS.

97

## 98 **2 Material and methods**

### 99 **2.1 Seawater collection**

100 Seawater samples were collected on-board the *R/V Bat-Galim* in 15 locations across the Israeli  
101 EEZ during August 2024 (Figure 1). Stations included coastal (close to shore, partly affected  
102 by perturbations and human activity, e.g., Rahav and Bar-Zeev, 2017; Raveh et al., 2019;  
103 Sisma-Ventura et al., 2022) and remote offshore (more pristine) locations. In each station,  
104 seawater was sampled at discrete depths between the surface (~0.5 m) and the bottom of the  
105 photic layer (~180 m) using Niskin bottles mounted on a rosette sampling system equipped  
106 with a Conductivity Temperature Depth (CTD) logger (Seabird 19 Plus), a fluorometer (Turner  
107 designs, Cyclops-7) and an oxygen optode (Seabird SBE 63). Water column samples were  
108 analyzed for dissolved inorganic nutrients (*i.e.*,  $\text{NO}_2+\text{NO}_3$ ,  $\text{PO}_4$ ), pico-phytoplankton  
109 abundance, size, biomass and primary production.



110

111 **Figure 1:** Map of the 15 sampling stations in the Levantine Basin, Eastern Mediterranean Sea.  
112 Stations extended along a coastal-to-offshore transect and were sampled in August 2024 aboard  
113 the R/V *Bat Galim*.

## 114 2.2 Inorganic nutrients

115 Pre-filtered (0.45  $\mu\text{m}$ ) samples were collected in acid-washed plastic tubes and were kept  
116 frozen at  $-20\text{ }^{\circ}\text{C}$  until analysis within a few months. Nutrients were measured with a Seal  
117 Analytical AA-3 system (Kress et al., 2014). Nitrate+nitrite ( $\text{NO}_2+\text{NO}_3$ ) was measured  
118 calorimetrically by Cd reduction and diazo dye (Kress et al., 2019). Orthophosphate ( $\text{PO}_4$ ) was  
119 determined using the molybdate blue method (Murphy and Riley, 1962). The precision for  
120  $\text{NO}_2+\text{NO}_3$  and  $\text{PO}_4$  was  $\pm 20\text{ nM}$  and  $3\text{ nM}$ , respectively. The limits of detection (two times the  
121 standard deviation of the blank) for  $\text{NO}_2+\text{NO}_3$  and  $\text{PO}_4$  were  $80\text{ nM}$  and  $8\text{ nM}$  respectively.  
122 The quality of the nutrient measurements was confirmed by the results of the inter-comparison  
123 exercises (JAPAN, QUASIMEME).

## 124 2.3 Chlorophyll-a (chl-a)

125 Seawater samples (300 ml) were concentrated using a Whatman Glass Fiber Filter, GF/F ( $\sim 0.7$   
126  $\mu\text{m}$  pore size) at low pressure ( $<150\text{ mbar}$ ) for chlorophyll-a (chl-a) analysis. The filters were  
127 placed in glass vials and frozen in the dark at  $-20\text{ }^{\circ}\text{C}$  until analysis. Chl-a pigment was extracted  
128 overnight in cold acetone (90%) in the dark and determined by the non-acidification method  
129 (Welschmeyer, 1994) using a Turner Designs (Trilogy) fluorometer.



#### 130 **2.4 Pico-phytoplankton abundance and size**

131 Bacterial abundance samples (1.8 ml) were fixed immediately after sampling with 6  $\mu$ l of  
132 microscopy-grade 50% glutaraldehyde after 10 min in the dark (0.2% final concentration,  
133 Sigma G-7651), frozen in liquid nitrogen and put at  $-80^{\circ}\text{C}$  until analysis. Analysis was  
134 performed using an Attune NxT Acoustic Focusing Flow Cytometer (Applied Biosystems),  
135 equipped with a syringe-based fluidic system and 488 and 405-nm lasers. Taxonomic  
136 discrimination was based on the orange fluorescence of phycoerythrin (585 nm) and the red  
137 fluorescence of Chl-a (630 nm), on side-scatter (SSC, a proxy of cell volume), and on forward-  
138 scatter (FSC, a proxy of cell size) (Marie et al., 1997). Prior to the analysis, fixed samples were  
139 fast thawed at  $37^{\circ}\text{C}$  water bath (Symphony) and the abundance of pico-phytoplankton (i.e.  
140 *Synechococcus*, *Prochlorococcus* and small eukaryotes) was determined.

141 The cell size distribution of the pico-phytoplankton communities was determined using flow  
142 cytometry based on FSC and side scatter SSC signals. The instrument was calibrated prior to  
143 each run using a mixture of fluorescent polystyrene microspheres of known diameters (0.2, 0.5,  
144 1.0, 3.0, and 10.0  $\mu\text{m}$ ; Applied Biosystems). These size-standard beads were run under the  
145 same flow cytometer settings as the samples, and their FSC and SSC signals were used to  
146 construct a calibration curve relating light scatter to particle size (Figure S1A). Additionally,  
147 21 random samples of  $\sim 300$  ml were concentrated onto polycarbonate GTTP filters (Millipore,  
148 0.2  $\mu\text{m}$  pore size) using support nitrocellulose filters below (Millipore, 0.47  $\mu\text{m}$  pore size) at  
149 low vacuum pressure ( $<150$  mmHg) to minimize cell deformation or rupture, fixed as above in  
150 a petri plate (0.2% glutaraldehyde final concentration) and analysed with a Nikon Eclipse 80i  
151 microscope equipped under x400 magnification within a few days. A minimum of 20 random  
152 fields of view per filter were examined, ensuring coverage of  $>100$  cells per sample. Size  
153 estimates were measured using ImageJ and were compared to the flow cytometry reads, which  
154 gave a good fit and a  $\sim 1:1$  slope ( $r^2=0.92$ ,  $n=21$ , Figure S1B).

#### 155 **2.5 Cellular nutrient quotas ( $Q_{\min}$ and $Q_{\max}$ ) and resource supply index (RSI)**

156 The theoretical cellular demand for nitrogen (N) and phosphorus (P) for the different pico-  
157 phytoplankton groups (i.e., *Synechococcus*, *Prochlorococcus* and pico-eukaryotes) was  
158 calculated based on the cells' diameter. These matrixes quantify the amount of a given nutrient  
159 required by a single cell to sustain metabolic processes and growth. Where,  $Q_{\min}$  represents the  
160 minimum cellular content of a nutrient that is necessary to maintain basic cellular functions  
161 and support balanced growth under ambient nutrient conditions (e.g., a "baseline"  
162 stoichiometric requirement that cannot be reduced without impairing growth). The  $Q_{\max}$  matrix



163 reflects the upper limit of nutrient storage capacity within a cell under replete (nutrient-rich)  
164 conditions. It represents the total nutrient content a cell can accumulate, including surplus  
165 stored beyond immediate metabolic needs (e.g., a ‘luxury uptake’).

166 Cell diameters ( $d$ ,  $\mu\text{m}$ ) were measured using the FSC signal in the flow cytometric analyses.  
167 Assuming spherical cell morphology, cell volume ( $V$ ,  $\mu\text{m}^3$ ) was calculated as shown in Eq. 1:

$$168 \quad (1) \quad V = \frac{\pi}{6} \times d^3$$

169 We then converted the cell’s volume to cellular carbon content ( $\text{fg C cell}^{-1}$ ) using the empirical  
170 allometric relationship derived by Menden-Deuer and Lessard, (2000) and shown in Eq. 2:

$$171 \quad (2) \quad \text{C content} = 0.216 \times V^{0.939}$$

172 The cellular N and P content were estimated from the cellular C content by using the canonical  
173 Redfield molar ratios ( $\text{C:N} = \sim 6.6:1$  and  $\text{C:P} = \sim 106:1$ , Redfield, 1934).

174 The calculated per-cell quotas were the  $Q_{\min}$  (i.e.,  $Q_{\min,\text{N}} = \text{N content}$  and  $Q_{\min,\text{P}} = \text{P content}$ ).  
175  $Q_{\max}$  was defined as twice  $Q_{\min}$  (Marañón et al., 2013).

176 The Resource Supply Index (RSI) integrates cellular nutrient demand with ambient nutrient  
177 availability to provide a dimensionless measure of nutrient sufficiency at the population level.  
178 RSI was calculated as shown in Eq. 3, defined as the ratio between the total nutrient  
179 concentration in the surrounding environment and the total cellular demand for that nutrient if  
180 all cells reached  $Q_{\max}$ .

$$181 \quad (3) \quad \text{RSI} = \frac{[\text{Ambient nutrient}]}{Q_{\max} \times \text{cell abundance}}$$

182 Where,  $\text{RSI} > 1$  indicate that ambient nutrient concentrations are theoretically sufficient to  
183 satisfy cellular nutrient requirements for the observed population size, whereas  $\text{RSI} < 1$  suggests  
184 that environmental supply is inadequate to meet cellular demand.

## 185 **2.6 Statistical analyses**

186 Principal Coordinates Analysis (PCoA) were generated based on Euclidean distance matrices  
187 to visualize patterns of multivariate environmental variation and to identify the principal  
188 gradients structuring the sampled water column. The analysis was performed on the  
189 standardized environmental matrix. Environmental variables were subsequently fitted as  
190 vectors (envfit approach) onto the ordination space, with vector direction indicating the  
191 gradient of increasing values and vector length representing the strength of correlation



192 (Pearson's  $r$ ) between each variable and the ordination axes. To examine how cell size  
193 variability is related to these environmental gradients, we projected the average cell diameter  
194 of *Synechococcus*, *Prochlorococcus*, and pico-eukaryotes onto the PCoA as passive vectors.  
195 This approach allowed us to assess the strength and direction of the correlation between cell  
196 size and the major environmental gradients without influencing the underlying ordination  
197 structure. Additionally, we quantified the proportion of size variability explained by the  
198 combined environmental matrix using multiple linear regression for each group, reporting the  
199 coefficient of determination ( $R^2$ ) as a measure of explanatory power. All multivariate analyses  
200 were conducted in Python (v3.10) using the numpy, pandas, and scikit-learn libraries, with  
201 visualization performed in matplotlib.

202

### 203 **3 Results**

#### 204 **3.1 Biogeochemical characteristics of the Low-Nutrient Low-Chlorophyll (LNL) EMS**

205 The water column was stratified with well defined water masses within the photic layer (Figure  
206 2A). The upper mixed layer depth (MLD) ranged from ~25-30 m, with Sigma-theta (density)  
207 of ~25-26  $\text{kg m}^{-3}$  and surface temperatures of ~28-30 °C. The water density increased with  
208 depth, reaching 28-29  $\text{kg m}^{-3}$  at the bottom of the photic layer (~180 m). Such a stable  
209 stratification minimizes nutrients replenishment from deeper depths lead to low, often below  
210 the detection levels, of inorganic nutrients (Figure 2B,C) and thus to low phytoplankton  
211 biomass represented by chlorophyll-*a* (Figure 2D). Surface water NO<sub>x</sub> (NO<sub>2</sub>+NO<sub>3</sub>) ranged  
212 from ~0.04  $\mu\text{mol L}^{-1}$  in the offshore water and increased near the coast fivefold; ~0.20  $\mu\text{mol L}^{-1}$   
213 (Figure 2B). NO<sub>x</sub> increased with depth and was >0.1-0.3  $\mu\text{mol L}^{-1}$  below ~100 m till the  
214 bottom of the photic zone (Figure 2B). These values, although higher than the very top surface  
215 water, are still considered low and representative of oligotrophic seas (Siokou-Frangou et al.,  
216 2010). Orthophosphate (PO<sub>4</sub>) was overall homogeneous throughout the water column, ranging  
217 from below detection (<0.008  $\mu\text{mol L}^{-1}$ ) to ~0.02  $\mu\text{mol L}^{-1}$  (Figure 2C). Nevertheless, the  
218 resulting N:P ratio was often higher than the 16:1 'Redfield ratio', suggesting N limiting  
219 conditions for phytoplankton. In agreement, the spatial distribution of chlorophyll mirrored  
220 that of NO<sub>x</sub> (Figure 2B vs. 2D), suggesting high dependence of phytoplankton to nitrogen  
221 species. Where, the surface chlorophyll concentrations were typically low (<0.1  $\mu\text{g L}^{-1}$ ) and  
222 increased with depth reaching maximal values around the Deep Chlorophyll Maxima (DCM)  
223 of ~0.3  $\mu\text{g L}^{-1}$  (Figure 2D). The location of the DCM in the water column changed westward  
224 and deepened from ~75 m in more coastal locations to ~140 m in the offshore (Figure 2D).



225 Together, these physiochemical and biological characteristics highlight the LNLC oligotrophic  
226 nature of the study area, in accordance with previous studies from the area (abovementioned  
227 references).

228

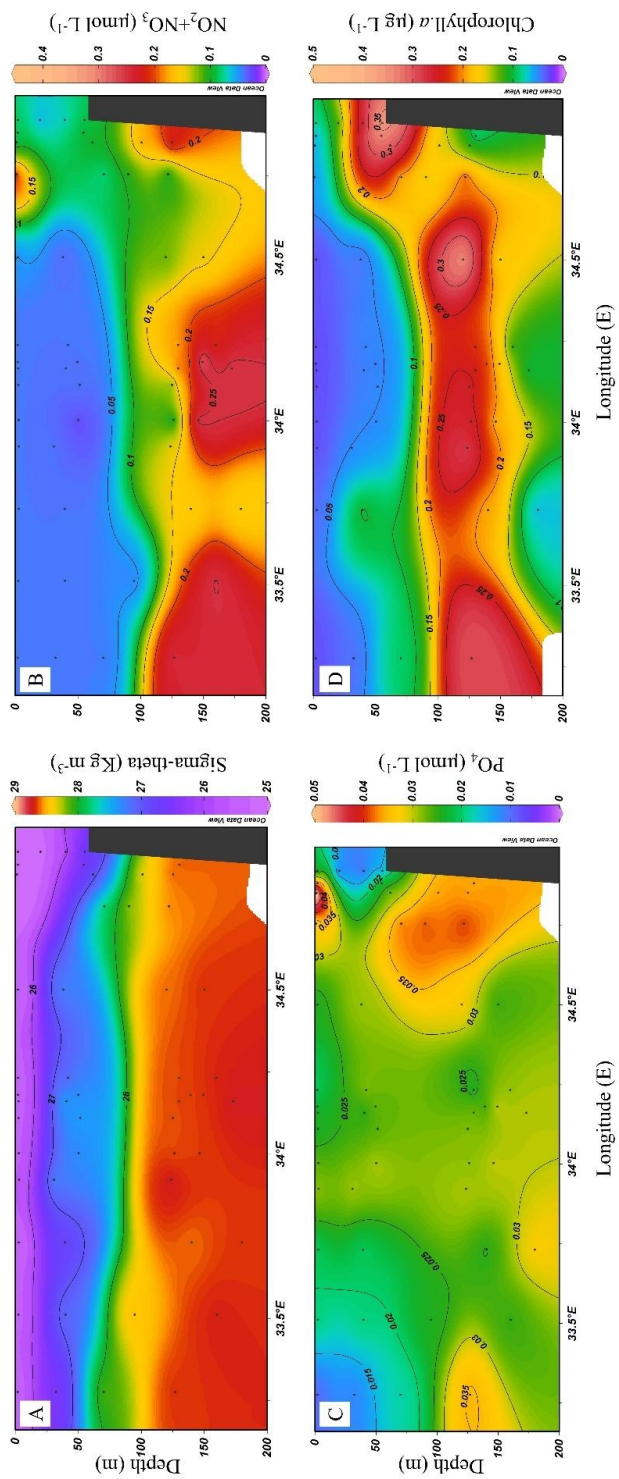
### 229 **3.2 Pico-phytoplankton cell size is an indicator for oligotrophy in the EMS**

230 Pico-phytoplankton communities consisted of the two cyanobacterial genera *Prochlorococcus*  
231 and *Synechococcus*, along with photoautotrophic pico-eukaryotic cells (Figure 3).  
232 *Synechococcus* was typically more abundant in surface waters (~20,000-25,000 cells ml<sup>-1</sup>) and  
233 in coastal stations (~25,000-60,000 cells ml<sup>-1</sup>) compared to the deeper water layers >100 m  
234 (~5,000-15,000 cells ml<sup>-1</sup>) (Figure 3A). Differently than its abundance, *Synechococcus*  
235 biovolume was generally smaller in the upper 100 m than in the 100-180 m layer, averaging  
236  $0.98 \pm 0.13 \mu\text{m}^3$  (range: 0.8-1.2  $\mu\text{m}^3$ ) in the surface layer vs.  $1.12 \pm 0.20 \mu\text{m}^3$  (range: 0.8-1.5  $\mu\text{m}^3$ )  
237 at depth (Figure 3B). Larger *Synechococcus* cells were found in coastal nutrient-richer water  
238 than in offshore oligotrophic regimes (Figure 4). *Prochlorococcus* was generally more  
239 abundant at the DCM, where its concentrations ranged from ~10,000 to ~80,000 cells ml<sup>-1</sup>  
240 compared to surface waters where they ranged from as low as ~1,000 cells ml<sup>-1</sup> to ~58,000 cells  
241 ml<sup>-1</sup> (Figure 3C). *Prochlorococcus* biovolume was smaller than that of *Synechococcus* and  
242 showed a clear increase with depth (Figure 3D). The average surface biovolume of  
243 *Prochlorococcus* was  $0.62 \pm 0.07 \mu\text{m}^3$  (range: 0.51-0.73  $\mu\text{m}^3$ ), increasing to  $0.68 \pm 0.04 \mu\text{m}^3$   
244 (range: 0.62-0.74  $\mu\text{m}^3$ ) at the DCM. No significant differences in *Prochlorococcus* cell  
245 biovolume were observed between coastal and offshore stations (Figure 4), thus suggest a lower  
246 cell plasticity compared to *Synechococcus* or pico-eukaryotes (discussion below). Pico-  
247 eukaryote abundance was generally higher in the upper 100 m (~100 to 3,700 cells ml<sup>-1</sup>)  
248 compared to deeper waters (below detection to ~1,100 cells ml<sup>-1</sup>), with consistently greater  
249 concentrations in coastal stations than offshore (Figure 3E). Generally, pico-eukaryotic cells  
250 were larger than of *Synechococcus* and *Prochlorococcus*, averaging ~1.9, 1.0 and 0.6  $\mu\text{m}^3$   
251 across all depths and stations, respectively. Nevertheless, pico-eukaryotes biovolume increased  
252 with depth (Figures 3F), as well as showed an increasing trend from coastal toward offshore  
253 waters (Figure 4). At the upper 100 m, pico-eukaryotes biovolume was  $\sim 1.75 \pm 0.37 \mu\text{m}^3$  (range:  
254 1.16-2.60  $\mu\text{m}^3$ ), while at 100-180 m it was  $2.07 \pm 0.48 \mu\text{m}^3$  (range: 1.15-2.95  $\mu\text{m}^3$ ).

255 Taken together, pico-phytoplankton dominated across different depths and water masses;  
256 however, all three groups exhibited overall similar vertical and spatial patterns in cell size with  
257 an increasing trend with depth, as well as from coastal toward offshore waters (Figures 3,4).  
258 These overarching trends mirrored the spatial distribution of nutrients, particularly NO<sub>x</sub>, and,



259 consequently, the distribution of chlorophyll (Figure 2). These observations suggest that cell  
260 size serves as a good environmental cue/indicator of oligotrophic conditions in the EMS and  
261 likely in other oceanic regimes (discussion below).

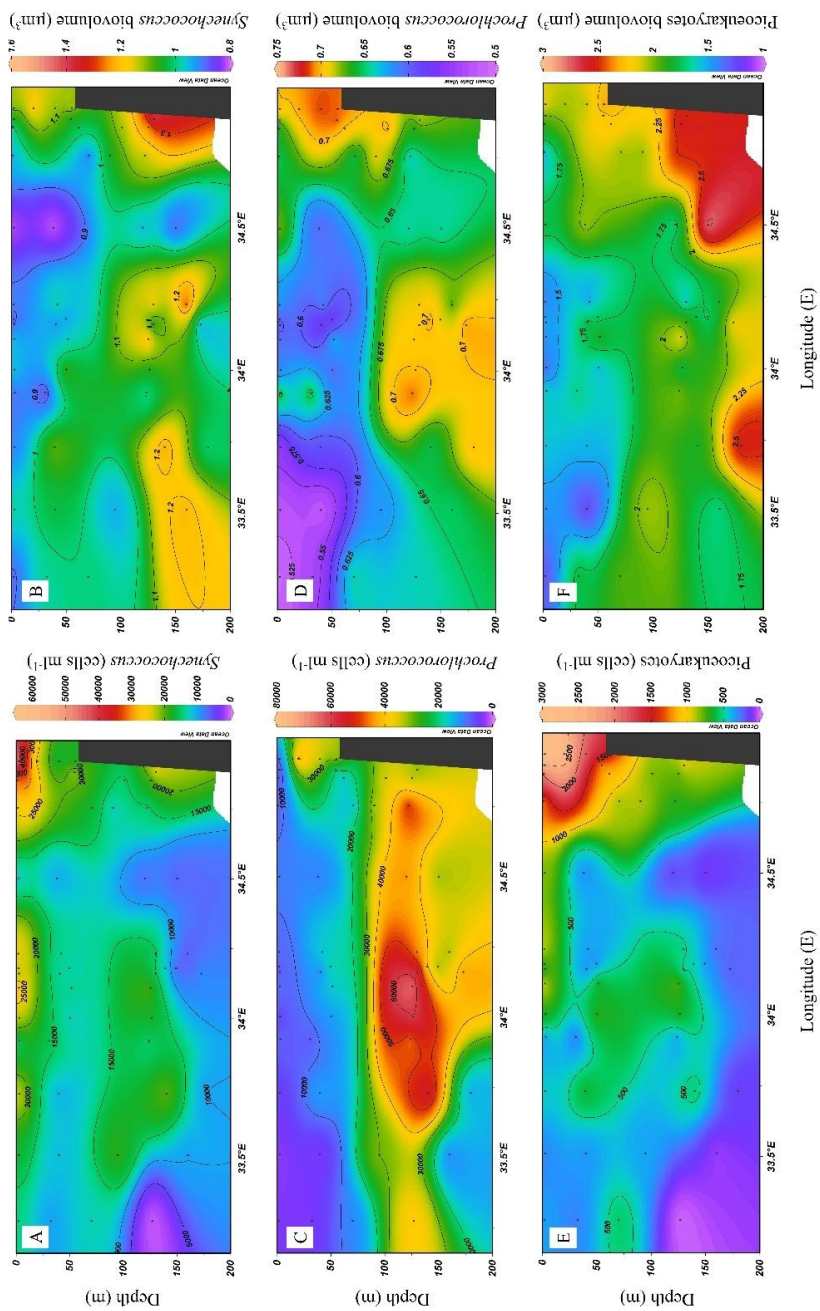


262

263 **Figure 2:** Spatial and depth patterns of Sigma-theta (A), dissolved  $\text{NO}_2+\text{NO}_3$  (B),  $\text{PO}_4$  (C) and chlorophyll.a (D) within the photic layer of the

264 Eastern Mediterranean Sea during summer 2024.

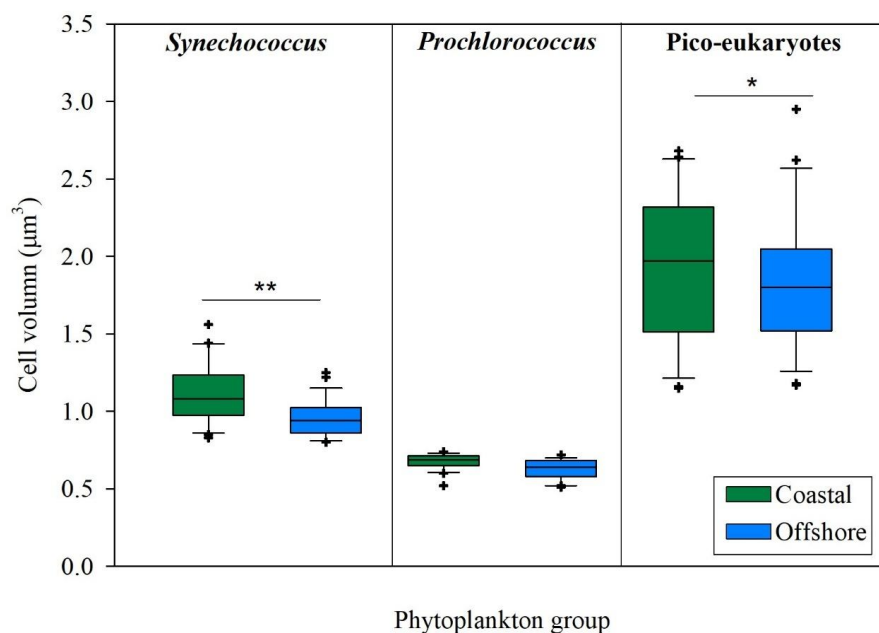
265



266

267 **Figure 3.** Spatial and depth patterns of *Synechococcus* (A,B), *Prochlorococcus* (C,D) and pico-eukaryotes (E,F) abundance (A,C,E) and  
268 biovolume (B,D,F) in the Eastern Mediterranean Sea during summer 2024.

12



269

270 **Figure 4:** Comparison of single-cell volumes ( $\mu\text{m}^3$ ) of *Synechococcus*, *Prochlorococcus*, and  
 271 pico-eukaryotes between coastal (green) and offshore (blue) waters in the Eastern  
 272 Mediterranean Sea. Box plots show the median, interquartile range, and overall distribution of  
 273 cell volumes. Statistically significant differences between coastal and offshore populations  
 274 were determined using Welch's *t*-tests or Mann–Whitney *U* tests. \*  $p < 0.05$ , \*\*  $p < 0.01$ .

275

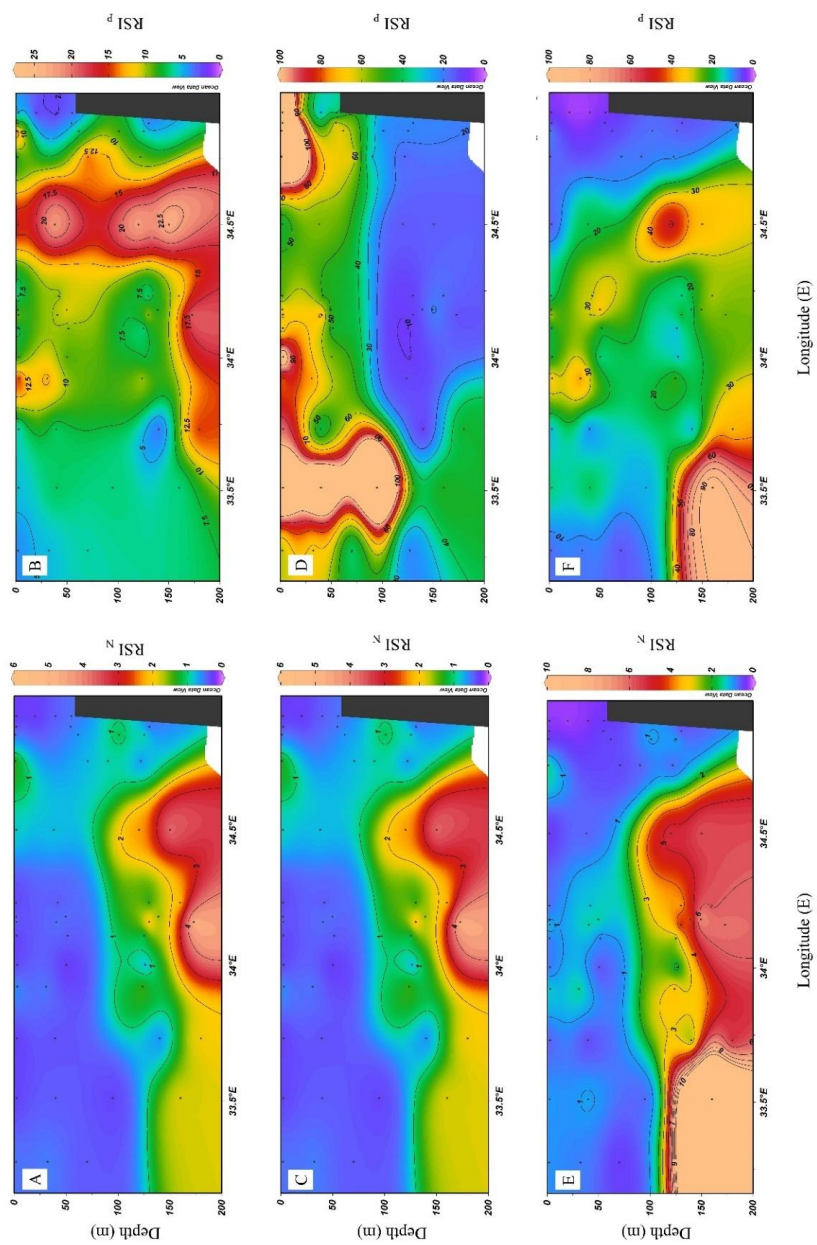
### 276 3.3 Can the ambient nutrients pool meet pico-phytoplankton's growth requirements?

277 Based on the cell's biovolume, abundance and the inorganic nutrient standing stocks we  
 278 calculated the per-cell quotas and RSI values of the three pico-phytoplankton populations in  
 279 the EMS (Marañón et al., 2014). These 'back of the envelope' calculations provided valuable  
 280 insights into the minimal and maximal nutrient requirements of the different pico-  
 281 phytoplankton cells and their theoretical nutrients limitations derived from cell size. Generally,  
 282 our results demonstrate that being a small cell have significant benefits in oligotrophic seas like  
 283 the EMS. Where, the relatively low  $Q_{\min}$  values of *Prochlorococcus* reflected its small cell size  
 284 and streamlined metabolic machinery, while *Synechococcus* and pico-eukaryotes exhibited  
 285 higher quotas due to their larger biomass and more complex cellular organization. These



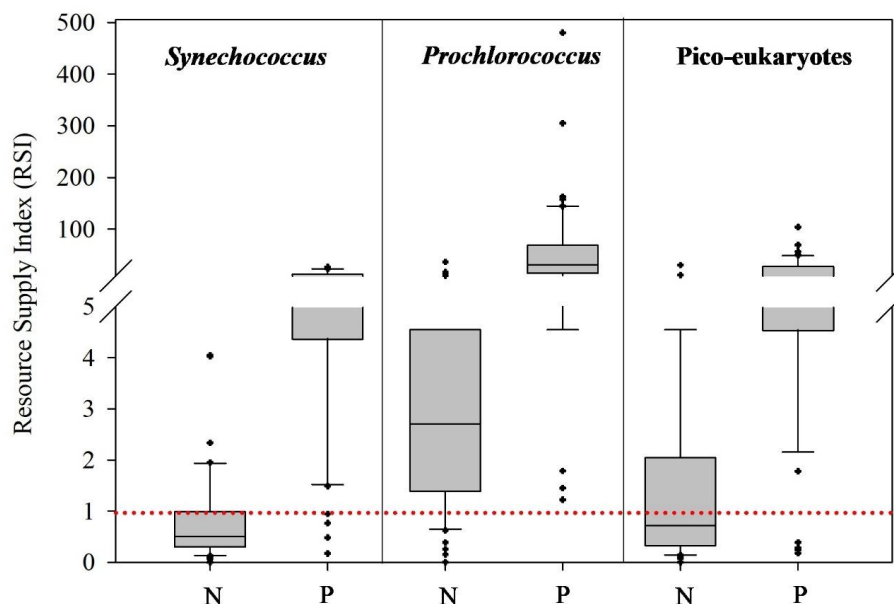
286 differences translated into distinct nutrient demands per cell and thus influence each group's  
287 ecological strategy and competitive capacity under the oligotrophic conditions of the EMS.

288 At the upper 100 m nitrogen supply was often below demand ( $RSI_n < 1$ ) for *Synechococcus* and  
289 pico-eukaryotes (Figure 5A,E) but not *Prochlorococcus* (Figure 5C) that lacks the genetic and  
290 enzymatic machinery required for  $NO_3$  assimilation (e.g., they do not carry the genes *narB* and  
291 often *nirA*, López-Lozano et al., 2002; Moore et al., 2002). Differently, the RSI values for  
292 phosphorus ( $RSI_p$ ) were larger than 1 in all pico-phytoplankton groups (Figure 5B,D,F). These  
293 results suggest that  $PO_4$  was not the main limiting nutrient for neither of the pico-phytoplankton  
294 groups and that N was the primary limiting element. Importantly, these results suggest  
295 physiological and ecological trade-offs among the pico-phytoplankton groups. Where,  
296 *Prochlorococcus* typically shows higher RSI values, and therefore a greater likelihood of  
297 sustaining growth due to its minimal nutrient requirements per cell, even under low-nutrient  
298 conditions. In contrast, *Synechococcus* and pico-eukaryotes frequently experience more severe  
299 N limitation (but to a lesser extent P based on RSI calculations), driven by higher per-cell  
300 quotas and large population standing stocks. Such differences in nutrient standing stocks likely  
301 contributed (along with other variables such as light intensities etc.) their depth distributions,  
302 seasonal dynamics, and competitive interactions in oligotrophic marine ecosystems.



303

304 **Figure 5:** A theoretical Resource Supply Index (RSI) of *Synechococcus* (A,B), *Prochlorococcus* (C,D) and pico-eukaryotes (E,F) calculated for  
305 NOx (A,C,E) and PO4 (B,D,F) in the Eastern Mediterranean Sea during summer 2024. RSI values <1 suggest nutrient limitation.



306

307 **Figure 6:** Box Whisker plots showing the data distribution of the RSI values for NO<sub>3</sub> and PO<sub>4</sub>  
 308 for the different pico-phytoplankton groups. The black line inside the box shows the median.  
 309 The dotted red line shows the RSI threshold, where RSI<1 imply on a nutrient limitation.

310

#### 311 4 Discussion

##### 312 4.1 Coastal-offshore variability in pico-phytoplankton cell size and abundance at the 313 EMS

314 Significant differences in pico-phytoplankton cell volumes were detected between coastal and  
 315 offshore waters, reflecting clear shifts in trait composition across environmental gradients.  
 316 Both *Synechococcus* and pico-eukaryotes exhibited larger mean cell volumes in nutrient-rich  
 317 coastal waters than in offshore environments. These differences in cell size are likely attributed  
 318 by human-induced perturbations typical to coastal water (e.g., Herut et al., 2024; Kress et al.,  
 319 2019; Rahav et al., 2020; Raveh et al., 2019) and reflects greater allocation to metabolic and  
 320 structural components, potentially improving competitive ability and storage capacity when  
 321 resources are not limiting. In contrast, *Prochlorococcus* displayed small and statistically weak  
 322 differences in cell volume between coastal and offshore stations. This minimal divergence  
 323 likely underscores the strong evolutionary and physiological constraints on this genus (e.g.,



324 Daakour et al., 2024), which remains highly specialized for life in chronically oligotrophic and  
325 stratified surface water. Its small and relatively invariant cell size reflects optimization for  
326 nutrient-poor conditions, where minimizing metabolic demands and maximizing surface-area-  
327 to-volume ratios provide a selective advantage.

328 The strong size structuring observed in the EMS is consistent with patterns reported from other  
329 marine oligotrophic systems such as the subtropical gyres, the Sargasso Sea, the North Pacific  
330 Subtropical Gyre (Station ALOHA), and the Red Sea (Buitenhuis et al., 2012; Coello-Camba  
331 and Agustí, 2021; Glover et al., 2007; Pearman et al., 2017). In all these regions, pico-  
332 phytoplankton dominate biomass and primary production, and small cell size is a defining  
333 adaptive trait under chronic nutrient scarcity. For example, in the North Pacific Subtropical  
334 Gyre, *Prochlorococcus* and small *Synechococcus* populations exhibit cell diameters and  
335 biomass comparable to those measured here and dominate where nitrate and phosphate are  
336 persistently near detection limits (Karl and Church, 2017; Winter et al., 2025). Similarly, the  
337 northern Red Sea shows depth-dependent increases in pico-phytoplankton cell size associated  
338 with nutricline proximity and the deep chlorophyll maximum (Rahav et al., 2015).

339 The EMS, however, represents one of the most phosphorus-depleted marine systems on Earth  
340 (Krom et al., 2010). While many subtropical gyres experience combined N and P limitation,  
341 the EMS is characterized by extremely low phosphate and high N:P ratios (Krom et al., 2005).  
342 Despite this, our RSI calculations show that phosphorus was not the primary limiting element  
343 for any of the pico-phytoplankton groups during summer, whereas nitrogen limitation was  
344 widespread for *Synechococcus* and pico-eukaryotes. This agrees with recent experimental and  
345 field studies in the EMS showing that nitrate availability often controls phytoplankton  
346 productivity during stratified periods even in coastal areas that have more NO<sub>3</sub> to begin with  
347 (Rahav et al., 2018).

348 Larger *Synechococcus* and pico-eukaryotes cell volumes requires higher cellular nitrogen and  
349 phosphorus quotas, which in the EMS frequently exceeded ambient nitrogen supply, as  
350 indicated by  $RSI_n < 1$ . This could explain, at least partly, why *Synechococcus* and pico-  
351 eukaryotes are often found in greater abundances in coastal water where nutrient inputs are  
352 higher (Kress et al., 2019). In contrast, *Prochlorococcus* remained largely unconstrained by  
353 both N and P, highlighting its exceptional adaptation to nutrient scarcity and/or that this  
354 cyanobacterium is limited by other nutrients such as organic molecules (e.g., urea, Hetharua et  
355 al., 2025; Moore et al., 2002; Zubkov et al., 2004). This physiological adaptation ‘allows’  
356 *Prochlorococcus* to dominate in the most nutrient-poor surface and warm water but also  
357 constrains its ecological niche: it is less competitive in nutrient-rich or turbulent environments



358 where larger phytoplankton with higher storage capacity and growth potential prevail (Billler  
359 et al., 2015; Partensky and Garczarek, 2010). Thus, we surmise that the weak spatial variation  
360 in *Prochlorococcus* cell size in the EMS reflects its highly specialized adaptation to the  
361 persistent ultra-oligotrophic conditions characterising this sea (Berman-Frank and Rahav,  
362 2012; Siokou-Frangou et al., 2010).

363 Taken together, the alterations in cellular size highlights important ecological implications.  
364 Where, larger cell volumes in *Synechococcus* and pico-eukaryotes not only enhance nutrient  
365 storage and metabolic potential but also increase their visibility to grazers and affect their  
366 position within microbial food webs (Charalampous et al., 2021; To et al., 2024; Ward et al.,  
367 2017). Such size shifts can therefore influence trophic transfer efficiency, carbon export  
368 potential, and the balance between autotrophic and heterotrophic processes. Conversely, the  
369 little/moderate change of *Prochlorococcus* cell size underscores its role as a persistent, small-  
370 celled specialist that dominates biomass and productivity in nutrient-depleted offshore regions.  
371 Collectively, these results demonstrate that cell size is a highly responsive functional trait that  
372 integrates environmental forcing with microbial community structure, revealing how resource  
373 availability and physical conditions shape ecosystem-level processes in oligotrophic marine  
374 systems such as the Eastern Mediterranean Sea.

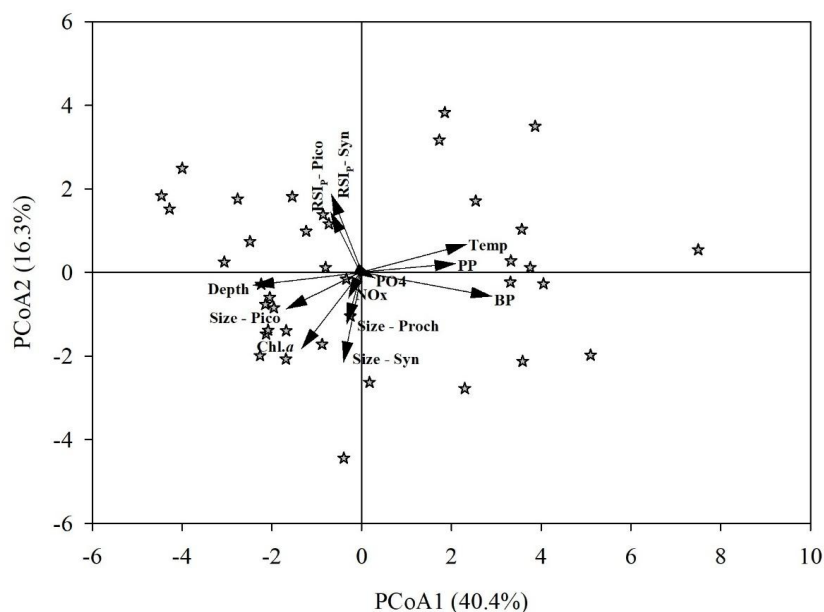
375

#### 376 **4.2 Environmental drivers explain a large fraction of cell-size variability in the EMS**

377 A multivariate ordination analysis reveals a relationship between *Synechococcus* cell size and  
378 the surrounding environmental gradients (Figure 7). The size vector for *Synechococcus* was  
379 closely aligned with NO<sub>3</sub> and PO<sub>4</sub> levels, as well as with chlorophyll.*a* concentrations that were  
380 greater in coastal water (Figure 2). This pattern indicates that *Synechococcus* cells tend to be  
381 larger under less oligotrophic conditions, often coinciding with regions of higher primary  
382 production (Raveh et al., 2015). These results are consistent with the ecological strategy of  
383 *Synechococcus*, which exhibits considerable physiological plasticity and is known to thrive in  
384 environments where higher nutrient supply ‘allows’ higher growth rates and increased cellular  
385 investment in metabolic machinery (Badger et al., 2006; Ungerer et al., 2018). Larger cell sizes  
386 under such conditions may reflect a shift toward improved nutrient storage capacity and  
387 enhanced uptake kinetics when compete (Garcia et al., 2016; Kerimoglu et al., 2012; Verdy et  
388 al., 2009). In contrast to *Synechococcus*, *Prochlorococcus* maintains smaller cell sizes under  
389 highly oligotrophic surface waters that prevail in the EMS during the summer (Ben-Ezra et al.,  
390 2021). The ‘tendency’ toward small cell size in such environments reflects *Prochlorococcus*’s



391 evolutionary optimization for efficient nutrient uptake and minimal metabolic cost under severe  
 392 resource limitation. Smaller cells possess a higher surface-area-to-volume ratio, which  
 393 enhances nutrient acquisition at nanomolar concentrations, and they require fewer resources  
 394 for cellular activities. Pico-eukaryotes cell size showed an intermediate response to  
 395 environmental variability. The size vector was most strongly associated with depth, PO<sub>4</sub>, and  
 396 chlorophyll.*a*, and to a lesser extent with NO<sub>3</sub> and temperature, indicating that picoeukaryote  
 397 size tends to increase under conditions of higher nutrient availability. This trend suggests that  
 398 pico-eukaryotes respond dynamically to shifts in resource supply and water column structure,  
 399 with larger cells occurring in environments that can support greater metabolic and structural  
 400 complexity.



401

402 **Figure 7:** Principal Coordinates Analysis (PCoA) of environmental gradients and their  
 403 relationship to pico-phytoplankton cell size in the oligotrophic Eastern Mediterranean Sea. The  
 404 ordination was performed using Euclidean distances based on standardized environmental  
 405 variables. Arrows represent the direction and strength (vector length) of correlations between  
 406 individual environmental variables and the first two PCoA axes (Axis 1 and Axis 2, which  
 407 together explain ~57% of total variance). Longer vectors indicate variables with stronger  
 408 correlations to the ordination space.



409

410 The patterns revealed by  $Q_{\min}$ ,  $Q_{\max}$ , and RSI analyses have important implications for how  
411 pico-phytoplankton communities may respond to future climate-driven changes in the marine  
412 environment. Ocean warming, enhanced stratification, and reduced vertical nutrient fluxes are  
413 expected to further intensify oligotrophic conditions in many subtropical and semi-enclosed  
414 basins (Ducklow and Doney, 2013). Such shifts will likely exacerbate phosphorus scarcity  
415 (Mansour et al., 2025) and increase the frequency and severity of N&P co-limitation (Browning  
416 and Moore, 2023), further constraining primary production and altering microbial food-web  
417 dynamics (Ibáñez et al., 2023). Species with lower nutrient requirements and greater  
418 physiological flexibility such as *Prochlorococcus* may therefore gain a competitive advantage  
419 under these conditions, potentially reshaping community composition and biogeochemical  
420 cycling. At the same time, changes in nutrient stoichiometry and supply ratios could modulate  
421 carbon export efficiency and the coupling between primary production and nutrient  
422 regeneration. Together, these findings underscore the value of cellular quota and RSI-based  
423 approaches not only for diagnosing present-day nutrient limitation but also for predicting  
424 ecosystem responses to future climate and nutrient regime shifts in oligotrophic ocean regions.  
425 Additionally, the spatial heterogeneity in cell physiology and biochemical composition can  
426 introduce systematic biases when converting pico-phytoplankton cell volume to carbon and  
427 nutrient quotas using a single universal conversion factor. Both laboratory and field studies  
428 show that cellular carbon density, chlorophyll content, and macromolecular composition in  
429 pico-phytoplankton may vary with nutrient regime, light availability, and growth rate (Finkel  
430 et al., 2010; Stawiarski et al., 2016; Wang et al., 2022). In nutrient-richer coastal waters and or  
431 in deeper water, these taxa tend to exhibit higher protein, pigment, and storage compound  
432 content per unit volume, leading to higher carbon and nutrient content for a given cell size than  
433 in oligotrophic offshore waters (Bertilsson et al., 2003; Givati et al., 2023; Liefer et al., 2019).  
434 Conversely, under extreme oligotrophy, cells are less pigmented, have lower ribosomal content  
435 (as they grow more slowly), and allocate a greater fraction of their volume to low-density  
436 structural components, resulting in lower carbon and nutrient quotas per unit volume (Fuszard  
437 et al., 2012; Hartmann et al., 2014). Applying a single global biovolume-to-carbon conversion  
438 factor across these contrasting environments would therefore overestimate offshore biomass  
439 and underestimate coastal biomass for *Synechococcus* and pico-eukaryotes and to a lesser  
440 extent *Prochlorococcus* that displays remarkably constrained cellular composition across  
441 environmental gradients (Figures 3-5). This is likely due to *Prochlorococcus*'s streamlined  
442 genome, reduced pigment suite, and tightly regulated cellular architecture. Together, applying



443 a single universal biovolume-to-carbon conversion across both coastal and offshore regimes  
444 and/or surface vs. deep water may introduce a biased biomass estimates of pico-phytoplankton  
445 in the oceans. Therefore, it is advised to measure pico-phytoplankton cell size along with its  
446 abundance.

## 447 **5 Conclusions**

448 This study highlights pico-phytoplankton cell size as a key functional trait linking nutrient  
449 scarcity to ecosystem-level carbon cycling in ultra-oligotrophic seas. Rather than abundance  
450 alone, size-dependent nutrient demand and physiological plasticity may determine which taxa  
451 will likely be dominating phytoplankton biomass under persistent nutrient limitation in the  
452 EMS. This size-structured trade-off has direct consequences for carbon fate, where dominance  
453 of very small cells promotes tight recycling within the microbial loop, reduces trophic transfer  
454 efficiency, and ultimately weakens the biological pump by limiting the formation of fast-  
455 sinking particles.

456 Additionally, our findings indicate that using a single, fixed carbon-per-cell conversion factor  
457 for each pico-phytoplankton group throughout the photic zone can introduce bias in depth-  
458 integrated biomass estimates in the EMS, and likely in other stratified oligotrophic oceans. We  
459 therefore recommend applying size-adjusted conversion factors of  $\sim 36\text{-}40$  fg C cell<sup>-1</sup> for  
460 surface and deep *Prochlorococcus*,  $\sim 255$  and  $\sim 290$  fg C cell<sup>-1</sup> for surface and deep  
461 *Synechococcus*, and  $\sim 2590$  and  $\sim 3050$  fg C cell<sup>-1</sup> for surface and deep pico-eukaryotes,  
462 respectively. Adoption of these depth-resolved factors will refine carbon standing stock  
463 assessments and enable more robust comparisons across coastal-offshore gradients and  
464 vertically structured oligotrophic systems.

465 Lastly, as ocean warming and enhanced stratification continue to expand low-nutrient, low-  
466 chlorophyll regions, selection for small cell size and low cellular quotas is likely to intensify.  
467 Such shifts are expected to promote recycling-dominated food webs, decoupling primary  
468 production from carbon export and reducing long-term carbon sequestration efficiency in  
469 oligotrophic oceans. Incorporating cell-size variability into biomass estimates and  
470 biogeochemical frameworks is therefore essential for predicting how future oceans will  
471 regulate carbon export under increasing stratification and nutrient decline.

472

473 *Author contributions.* Elad Albagly - formal analysis, investigation, methodology, writing  
474 original draft. Eyal Rahav - funding acquisition, resources, supervision, conceptualisation, data



475 curation, formal analysis, investigation, methodology, project administration, writing original  
476 draft.

477 *Data availability.* The data are presented in full in the main text or the supplementary material.  
478 The hydrographic data is openly available from <https://isramar.ocean.org.il/isramar2009/>.

479 *Competing interests.* None of the authors has any competing interests.

480 *Acknowledgements.* We would like to thank the R.V. *Bat-Galim* captain and crew for help at  
481 sea. This work is in partial fulfilment of Elad Albagly studies at the Hebrew University.

482 *Financial support.* The research was supported by the Israeli National monitoring program of  
483 the eastern Mediterranean Sea to Eyal Rahav.

#### 484 **References**

485 Alvain, S., Moulin, C., Dandonneau, Y., and Breon, F. .: Remote sensing of phytoplankton  
486 groups in case 1 waters from global SeaWiFS imagery, *Deep Sea Res. Part I Oceanogr. Res.*  
487 *Pap.*, 52, 1989–2004, <https://doi.org/10.1016/j.dsr.2005.06.015>, 2005.

488 Badger, M. R., Price, G. D., Long, B. M., and Woodger, F. J.: The environmental plasticity  
489 and ecological genomics of the cyanobacterial CO<sub>2</sub> concentrating mechanism, *J. Exp. Bot.*,  
490 57, 249–265, <https://doi.org/10.1093/jxb/eri286>, 2006.

491 Banse, K.: Cell volumes, maximal growth rates of unicellular algae and ciliates, and the role  
492 of ciliates in the marine pelagial, *Limnol. Oceanogr.*, 27, 1059–1071,  
493 <https://doi.org/10.4319/lo.1982.27.6.1059>, 1982.

494 Beardall, J., Stojkovic, S., and Larsen, S.: Living in a high CO<sub>2</sub> world: impacts of global  
495 climate change on marine phytoplankton, *Plant Ecol. Divers.*, 2, 191–205,  
496 <https://doi.org/10.1080/17550870903271363>, 2017.

497 Belkin, N., Guy-haim, T., Rubin-blum, M., Lazar, A., and Sisma-, G.: Influence of cyclonic  
498 and anti-cyclonic eddies on plankton biomass , activity and diversity in the southeastern  
499 Mediterranean Sea, 1–56, 2022.

500 Ben-Ezra, T., Krom, M. D., Tsemel, A., Berman-Frank, I., Herut, B., Lehahn, Y., Rahav, E.,  
501 Reich, T., Thingstad, T. F., and Sher, D.: Seasonal nutrient dynamics in the P depleted  
502 Eastern Mediterranean Sea, *Deep. Res. Part I*, 176, 103607,  
503 <https://doi.org/10.1016/j.dsr.2021.103607>, 2021.

504 Berman-Frank, I. and Rahav, E.: Nitrogen fixation as a source for new production in the  
505 Mediterranean Sea: a review, in: *Life in the Mediterranean Sea: A Look at Habitat Changes*,  
506 Nova Science Publishers, NY, 199–226, 2012.



507 Bertilsson, S., Berglund, O., Karl, D. M., and Chisholm, S. W.: Elemental composition of  
508 marine Prochlorococcus and Synechococcus: Implications for the ecological stoichiometry of  
509 the sea, *Limnol. Oceanogr.*, 48, 1721–1731, <https://doi.org/10.4319/lo.2003.48.5.1721>, 2003.  
510 Biller, S. J., Berube, P. M., Lindell, D., and Chisholm, S. W.: Prochlorococcus: the structure  
511 and function of collective diversity, *Nat. Rev. Microbiol.*, 13, 13–27,  
512 <https://doi.org/10.1038/nrmicro3378>, 2015.  
513 Boyd, P. W. and Trull, T. W.: Understanding the export of biogenic particles in oceanic  
514 waters: Is there consensus?, *Prog. Oceanogr.*, 72, 276–312,  
515 <https://doi.org/https://doi.org/10.1016/j.pocean.2006.10.007>, 2007.  
516 Browning, T. J. and Moore, C. M.: Global analysis of ocean phytoplankton nutrient limitation  
517 reveals high prevalence of co-limitation, *Nat. Commun.*, 14, 1–12,  
518 <https://doi.org/10.1038/s41467-023-40774-0>, 2023.  
519 Buitenhuis, E. T., Li, W. K. W., Lomas, M. W., Karl, D. M., Landry, M. R., and Jacquet, S.:  
520 Bacterial biomass distribution in the global ocean, *Earth Syst. Sci. Data*, 5, 301–315,  
521 <https://doi.org/10.5194/essdd-5-301-2012>, 2012.  
522 Charalampous, E., Matthiessen, B., and Sommer, U.: Grazing induced shifts in phytoplankton  
523 cell size explain the community response to nutrient supply, *Microorganisms*, 9, 2440,  
524 <https://doi.org/10.3390/microorganisms9122440>, 2021.  
525 Chisholm, S. W.: Phytoplankton size, in: *Primary Productivity and Biogeochemical Cycles in*  
526 *the Sea*, edited by: Falkowski, P. G., Woodhead, A. D., and Vivirito, K., Springer US,  
527 Boston, MA, 213–237, [https://doi.org/10.1007/978-1-4899-0762-2\\_12](https://doi.org/10.1007/978-1-4899-0762-2_12), 1992.  
528 Chisholm, S. W.: Stirring times in the Southern Ocean, *Nature*, 407, 685–687,  
529 <https://doi.org/10.1038/35037696>, 2000.  
530 Chkili, O., Meddeb, M., Mejri Kousri, K., Ben Garali, S. M., Makhlof Belkhalia, N.,  
531 Tedetti, M., Pagano, M., Belaaj Zouari, A., Belhassen, M., Niquil, N., and Sakka Hlaili, A.:  
532 Influence of nutrient gradient on phytoplankton size structure, primary production and carbon  
533 transfer pathway in a highly productive area (SE Mediterranean), *Ocean Sci. J.*, 58, 2023.  
534 Coello-Camba, A. and Agustí, S.: Picophytoplankton niche partitioning in the warmest  
535 oligotrophic sea, *Front. Mar. Sci.*, 8, 651877, <https://doi.org/10.3389/fmars.2021.651877>,  
536 2021.  
537 Daakour, S., Nelson, D. R., Fu, W., Jaiswal, A., Dohai, B., Alzahmi, A. S., Koussa, J.,  
538 Huang, X., Shen, Y., Twizere, J. C., and Salehi-Ashtiani, K.: Adaptive evolution signatures  
539 in Prochlorococcus: open reading frame (ORF)ome resources and insights from comparative  
540 genomics, *Microorganisms*, 12, 1–21, <https://doi.org/10.3390/microorganisms12081720>,



- 541 2024.
- 542 Ducklow, H. W. and Doney, S. C.: What is the metabolic state of the oligotrophic ocean? A  
543 debate., *Ann. Rev. Mar. Sci.*, 5, 525–33, [https://doi.org/10.1146/annurev-marine-121211-](https://doi.org/10.1146/annurev-marine-121211-172331)  
544 172331, 2013.
- 545 Falkowski, P.: Evolution of the nitrogen cycle and its influence on the biological  
546 sequestration of CO<sub>2</sub> in the ocean, *Nature*, 387, 272–275, 1997.
- 547 Field, C. B., Behrenfeld, M. J., Randerson, J. T., and Falkowski, P.: Primary Production of  
548 the Biosphere: Integrating Terrestrial and Oceanic Components, *Science* (80-. ), 281, 237–  
549 240, <https://doi.org/10.1126/science.281.5374.237>, 1998.
- 550 Finkel, Z. V., Beardall, J., Flynn, K. J., Quigg, A., Rees, T. A. V, and Raven, J. A.:  
551 Phytoplankton in a changing world: Cell size and elemental stoichiometry, *J. Plankton Res.*,  
552 32, 119–137, <https://doi.org/10.1093/plankt/fbp098>, 2010a.
- 553 Finkel, Z. V, Beardall, J., Flynn, K. J., Quigg, A., Rees, T. A. V, and Raven, J. A.:  
554 Phytoplankton in a changing world: cell size and elemental stoichiometry, *J. Plankton Res.*,  
555 32, 119–137, <https://doi.org/10.1093/plankt/fbp098>, 2010b.
- 556 Flombaum, P., Gallegos, J. L., Gordillo, R. a, Rincón, J., Zabala, L. L., Jiao, N., Karl, D. M.,  
557 Li, W. K. W., Lomas, M. W., Veneziano, D., Vera, C. S., Vrugt, J. a, and Martiny, A. C.:  
558 Present and future global distributions of the marine Cyanobacteria *Prochlorococcus* and  
559 *Synechococcus*., *Proc. Natl. Acad. Sci. U. S. A.*, 110, 9824–9,  
560 <https://doi.org/10.1073/pnas.1307701110>, 2013.
- 561 Fuszard, M. A., Wright, P. C., and Biggs, C. A.: Comparative quantitative proteomics of  
562 *prochlorococcus* ecotypes to a decrease in environmental phosphate concentrations., *Aquat.*  
563 *Biosyst.*, 8, 7, <https://doi.org/10.1186/2046-9063-8-7>, 2012.
- 564 Garcia, N. S., Bonachela, J. A., and Martiny, A. C.: Interactions between growth-dependent  
565 changes in cell size, nutrient supply and cellular elemental stoichiometry of marine  
566 *Synechococcus*, *ISME J.*, 10, 2715–2724, <https://doi.org/10.1038/ismej.2016.50>, 2016.
- 567 Geider, R., Piatt, T., and Raven, J.: Size dependence of growth and photosynthesis in  
568 diatoms: a synthesis, *Mar. Ecol. Prog. Ser.*, 30, 93–104, <https://doi.org/10.3354/meps030093>,  
569 1986.
- 570 Givati, S., Yang, X., Sher, D., and Rahav, E.: Testing the growth rate and  
571 translation compensation hypotheses in marine bacterioplankton, *Environ. Microbiol.*, 25,  
572 1186–1199, <https://doi.org/10.1111/1462-2920.16346>, 2023.
- 573 Glover, H. E., Garside, C., and Trees, C. C.: Physiological responses of Sargasso Sea  
574 picoplankton to nanomolar nitrate perturbations, *J. Plankton Res.*, 29, 263–274,



- 575 <https://doi.org/10.1093/plankt/fbm013>, 2007.
- 576 Guidi, L., Stemann, L., Jackson, G. A., Ibanez, F., Claustre, H., Legendre, L., Picheral, M.,  
577 and Gorsky, G.: Effects of phytoplankton community on production, size and export of large  
578 aggregates: A world-ocean analysis, *Limnol. Oceanogr.*, 54, 1951–1963,  
579 <https://doi.org/10.4319/lo.2009.54.6.1951>, 2009.
- 580 Hartmann, M., Gomez-Pereira, P., Grob, C., Ostrowski, M., Scanlan, D. J., and Zubkov, M.  
581 V: Efficient CO<sub>2</sub> fixation by surface *Prochlorococcus* in the Atlantic Ocean., *ISME J.*, 8,  
582 2280–9, <https://doi.org/10.1038/ismej.2014.56>, 2014.
- 583 Herut, B., Goldman, R., Ozer, T., Lazar, A., Biton, E., Gertman, I., Silverman, J., Segal, Y.,  
584 Sisma-Ventura, G., Gertner, Y., Rubin-Blum, M., Belkin, N., and Rahav, E.: Tar pollution  
585 event (2021) at the Southeastern Levantine oligotrophic basin, short-term impacts and  
586 operational oceanography perspectives, *Mar. Pollut. Bull.*, 198, 115892,  
587 <https://doi.org/10.1016/j.marpolbul.2023.115892>, 2024.
- 588 Hetharua, B., Xu, M., Sun, S., Zhang, K., Yang, H., Liu, H., and Kao, S.-J.: Temperature-  
589 driven nitrogen mixotrophy shapes marine cyanobacteria *Prochlorococcus* and  
590 *Synechococcus* latitudinal distribution pattern, *Commun. Earth Environ.*, 6, 149,  
591 <https://doi.org/10.1038/s43247-025-02102-w>, 2025.
- 592 Huang, Y., Nicholson, D., Huang, B., and Cassar, N.: Global estimates of marine gross  
593 primary production based on machine learning upscaling of field observations, *Global*  
594 *Biogeochem. Cycles*, 35, e2020GB006718,  
595 <https://doi.org/10.1029/2020GB006718>, 2021.
- 596 Ibáñez, C., Caiola, N., Barquín, J., Belmar, O., Benito-Granell, X., Casals, F., Fennessy, S.,  
597 Hughes, J., Palmer, M., Peñuelas, J., Romero, E., Sardans, J., and Williams, M.: Ecosystem-  
598 level effects of re-oligotrophication and N:P imbalances in rivers and estuaries on a global  
599 scale, *Glob. Chang. Biol.*, 29, 1248–1266, <https://doi.org/10.1111/gcb.16520>, 2023.
- 600 Karl, D. M. and Church, M. J.: Ecosystem structure and dynamics in the North Pacific  
601 Subtropical Gyre: new views of an old ocean, *Ecosystems*, 20, 433–457,  
602 <https://doi.org/10.1007/s10021-017-0117-0>, 2017.
- 603 Kerimoglu, O., Straile, D., and Peeters, F.: Role of phytoplankton cell size on the competition  
604 for nutrients and light in incompletely mixed systems, *J. Theor. Biol.*, 300, 330–343,  
605 <https://doi.org/10.1016/j.jtbi.2012.01.044>, 2012.
- 606 Kiørboe, T.: Turbulence, phytoplankton cell size, and the structure of pelagic food webs,  
607 *Adv. Mar. Biol.*, 29, 1–72, [https://doi.org/10.1016/S0065-2881\(08\)60129-7](https://doi.org/10.1016/S0065-2881(08)60129-7),  
608 1993.



- 609 Kress, N., Gertman, I., and Herut, B.: Temporal evolution of physical and chemical  
610 characteristics of the water column in the Easternmost Levantine Basin (Eastern  
611 Mediterranean Sea) from 2002 to 2010, *J. Mar. Syst.*, 135, 6–13,  
612 <https://doi.org/10.1016/j.jmarsys.2013.11.016>, 2014.
- 613 Kress, N., Rahav, E., Silverman, J., and Herut, B.: Environmental status of Israel's  
614 Mediterranean coastal waters: Setting reference conditions and thresholds for nutrients,  
615 chlorophyll-a and suspended particulate matter, *Mar. Pollut. Bull.*, 141, 612–620,  
616 <https://doi.org/10.1016/j.marpolbul.2019.02.070>, 2019.
- 617 Krom, M., Kress, N., Berman-Frank, I., and Rahav, E.: Past, present and future patterns in the  
618 nutrient chemistry of the eastern mediterranean, [https://doi.org/10.1007/978-94-007-6704-](https://doi.org/10.1007/978-94-007-6704-1_4)  
619 [1\\_4](https://doi.org/10.1007/978-94-007-6704-1_4), 2013.
- 620 Krom, M. D., Woodward, E. M. S., Herut, B., Kress, N., Carbo, P., Mantoura, R. F. C.,  
621 Spyres, G., Thingsted, T. F., Wassmann, P., Wexels-Riser, C., Kitidis, V., Law, C., and  
622 Zodiatis, G.: Nutrient cycling in the south east Levantine basin of the eastern Mediterranean:  
623 Results from a phosphorus starved system, *Deep. Res. Part II Top. Stud. Oceanogr.*, 52,  
624 2879–2896, <https://doi.org/10.1016/j.dsr2.2005.08.009>, 2005.
- 625 Krom, M. D., Emeis, K.-C., and Van Cappellen, P.: Why is the Eastern Mediterranean  
626 phosphorus limited?, *Prog. Oceanogr.*, 85, 236–244,  
627 <https://doi.org/10.1016/j.pocean.2010.03.003>, 2010.
- 628 Liefer, J. D., Garg, A., Fyfe, M. H., Irwin, A. J., Benner, I., Brown, C. M., Follows, M. J.,  
629 Omta, A. W., and Finkel, Z. V.: The macromolecular basis of phytoplankton C:N:P under  
630 nitrogen starvation, *Front. Microbiol.*, 10, 763, <https://doi.org/10.3389/fmicb.2019.00763>,  
631 2019.
- 632 Lindell, D. and Post, A. F.: Ultraphytoplankton succession is triggered by deep winter mixing  
633 in the Gulf of Aqaba (Eilat), Red Sea, *Limnol. Oceanogr.*, 40, 1130–1141,  
634 <https://doi.org/10.4319/lo.1995.40.6.1130>, 1995.
- 635 Litchman, E. and Klausmeier, C. A.: Trait-based community ecology of phytoplankton,  
636 *Annu. Rev. Ecol. Evol. Syst.*, 39, 615–639,  
637 <https://doi.org/10.1146/annurev.ecolsys.39.110707.173549>, 2008.
- 638 López-Lozano, A., Diez, J., Alaoui, S., Moreno-Vivián, C., and García-Fernández, J. M.:  
639 Nitrate is reduced by heterotrophic bacteria but not transferred to *Prochlorococcus* in non-  
640 axenic cultures, *FEMS Microbiol. Ecol.*, 41, 151–160, [https://doi.org/10.1111/j.1574-](https://doi.org/10.1111/j.1574-6941.2002.tb00976.x)  
641 [6941.2002.tb00976.x](https://doi.org/10.1111/j.1574-6941.2002.tb00976.x), 2002.
- 642 Mansour, A. A., Gholmieh, L. M., Gholmieh, E. C., Duan, R., Bian, X., Chen, Y., John, S.



- 643 G., Hutchins, D. A., and Fu, F.-X.: Phosphorus limitation heightens vulnerability of  
644 *Crocospaera watsonii* to ocean warming compared with iron limitation, *Front. Microbiol.*,  
645 16, 1718897, <https://doi.org/10.3389/fmicb.2025.1718897>, 2025.
- 646 Maranon, E.: Cell size as a key determinant of phytoplankton metabolism and community  
647 structure, *Ann. Rev. Mar. Sci.*, 7, 241–264, <https://doi.org/10.1146/annurev-marine-010814-015955>, 2015.
- 649 Maranon, E., Cermeno, P., Huete-Ortega, M., Lopez-Sandoval, D. C., Mourino-Carballido,  
650 B., and Rodriguez-Ramos, T.: Resource supply overrides temperature as a controlling factor  
651 of marine phytoplankton growth, *PLoS One*, 9, 20–23,  
652 <https://doi.org/10.1371/journal.pone.0099312>, 2014.
- 653 Marañón, E., Cermeño, P., López-Sandoval, D. C., Rodríguez-Ramos, T., Sobrino, C., Huete-  
654 Ortega, M., Blanco, J. M., and Rodríguez, J.: Unimodal size scaling of phytoplankton growth  
655 and the size dependence of nutrient uptake and use, *Ecol. Lett.*, 16, 371–379,  
656 <https://doi.org/10.1111/ele.12052>, 2013.
- 657 Marie, D., Partensky, F., Jacquet, S., and Vaultot, D.: Enumeration and cell cycle analysis of  
658 natural populations of marine picoplankton by flow cytometry using the nucleic acid stain  
659 SYBR Green I, *Appl. Environ. Microbiol.*, 63, 186–193, 1997.
- 660 Menden-Deuer, S. and Lessard, E. J.: Carbon to volume relationships for dinoflagellates,  
661 diatoms, and other protist plankton, *Limnol. Oceanogr.*, 45, 569–579,  
662 <https://doi.org/https://doi.org/10.4319/lo.2000.45.3.0569>, 2000.
- 663 Moore, L. R., Post, A. F., Rocop, G., and Chisholm, S. W.: Utilization of different nitrogen  
664 sources by the marine cyanobacteria *Prochlorococcus* and *Synechococcus*, *Limnol.*  
665 *Oceanogr.*, 47, 989–996, <https://doi.org/https://doi.org/10.4319/lo.2002.47.4.0989>, 2002.
- 666 Murphy, J. and Riley, J. P.: A modified single solution method for the determination of  
667 phosphate in natural waters, *Anal. Chim. Acta*, 27, 31–36,  
668 [https://doi.org/https://doi.org/10.1016/S0003-2670\(00\)88444-5](https://doi.org/https://doi.org/10.1016/S0003-2670(00)88444-5), 1962.
- 669 Partensky, F. and Garczarek, L.: *Prochlorococcus*: Advantages and Limits of Minimalism,  
670 *Ann. Rev. Mar. Sci.*, 2, 305–331, <https://doi.org/10.1146/annurev-marine-120308-081034>,  
671 2010.
- 672 Pearman, J. K., Ellis, J., Irigoien, X., Sarma, Y. V. B., Jones, B. H., and Carvalho, S.:  
673 Microbial planktonic communities in the Red Sea: high levels of spatial and temporal  
674 variability shaped by nutrient availability and turbulence, *Sci. Rep.*, 7, 1–15,  
675 <https://doi.org/10.1038/s41598-017-06928-z>, 2017.
- 676 Rahav, E. and Bar-Zeev, E.: Sewage outburst triggers *Trichodesmium* bloom and enhance N<sub>2</sub>



- 677 fixation rates, *Sci. Rep.*, 7, 4367, <https://doi.org/10.1038/s41598-017-04622-8>, 2017.
- 678 Rahav, E. and Berman-Frank, I.: Temporal and vertical dynamics of diatoms and  
679 dinoflagellates in the southeastern Mediterranean Sea, *J. Plankton Res.*, 1–11,  
680 <https://doi.org/10.1093/plankt/fbad025>, 2023.
- 681 Rahav, E., Herut, B., Stambler, N., Bar-Zeev, E., Mulholland, M. R., and Berman-Frank, I.:  
682 Uncoupling between dinitrogen fixation and primary productivity in the eastern  
683 Mediterranean Sea, *J. Geophys. Res. Biogeosciences*, 118, 195–202,  
684 <https://doi.org/10.1002/jgrg.20023>, 2013.
- 685 Rahav, E., Herut, B., Mulholland, M., Belkin, N., Elifantz, H., and Berman-Frank, I.:  
686 Heterotrophic and autotrophic contribution to dinitrogen fixation in the Gulf of Aqaba, *Mar.*  
687 *Ecol. Prog. Ser.*, 522, 67–77, <https://doi.org/10.3354/meps11143>, 2015.
- 688 Rahav, E., Raveh, O., Hazan, O., Gordon, N., Kress, N., Silverman, J., and Herut, B.: Impact  
689 of nutrient enrichment on productivity of coastal water along the SE Mediterranean shore of  
690 Israel - A bioassay approach, *Mar. Pollut. Bull.*, 127, 559–567,  
691 <https://doi.org/10.1016/j.marpolbul.2017.12.048>, 2018.
- 692 Rahav, E., Raveh, O., Yanuka-Golub, K., Belkin, N., Astrahan, P., Maayani, M., Tsumi, N.,  
693 Kiro, Y., Herut, B., Silverman, J., and Angel, D. L.: Nitrate-enrichment structures  
694 phytoplankton communities in the shallow Eastern Mediterranean coastal waters, *Front. Mar.*  
695 *Sci.*, 7, 1–13, <https://doi.org/10.3389/fmars.2020.611497>, 2020.
- 696 Raveh, O., David, N., Rilov, G., and Rahav, E.: The temporal dynamics of coastal  
697 phytoplankton and bacterioplankton in the Eastern Mediterranean Sea, *PLoS One*, 10, 1–23,  
698 <https://doi.org/10.1371/journal.pone.0140690>, 2015.
- 699 Raveh, O., Angel, D. L., Astrahan, P., Belkin, N., Bar-Zeev, E., and Rahav, E.:  
700 Phytoplankton response to N-rich well amelioration brines: A mesocosm study from the  
701 southeastern Mediterranean Sea, *Mar. Pollut. Bull.*, 146, 355–365,  
702 <https://doi.org/10.1016/j.marpolbul.2019.06.067>, 2019.
- 703 Raven, J. A.: The twelfth tansley lecture. Small is beautiful: the picophytoplankton, *Funct.*  
704 *Ecol.*, 12, 503–513, <https://doi.org/https://doi.org/10.1046/j.1365-2435.1998.00233.x>, 1998.
- 705 Redfield, A.: On the proportions of organic derivatives in sea water and their relation to the  
706 composition of phytoplankton, in: James Johnstone Memorial Volume, edited by: R. J.  
707 Daniel, University Press of Liverpool, Liverpool, 177–192, 1934.
- 708 Reich, T., Ben-ezra, T., Belkin, N., Tsemel, A., Aharonovich, D., Roth-rosenberg, D., Givati,  
709 S., Bialik, M., Herut, B., Berman-frank, I., Frada, M., Krom, M. D., Lehahn, Y., Rahav, E.,  
710 and Sher, D.: A year in the life of the Eastern Mediterranean : Monthly dynamics of



- 711 phytoplankton and bacterioplankton in an ultra-oligotrophic sea, *Deep. Res. Part I*, 182,  
712 103720, <https://doi.org/10.1016/j.dsr.2022.103720>, 2022.
- 713 Reich, T., Belkin, N., Sisma-Ventura, G., Berman-Frank, I., and Rahav, E.: Significant dark  
714 inorganic carbon fixation in the euphotic zone of an oligotrophic sea, *Limnol. Oceanogr.*,  
715 9999, 1–14, <https://doi.org/10.1002/lno.12560>, 2024.
- 716 Siokou-Frangou, I., Christaki, U., Mazzocchi, M. G., Montresor, M., Ribera d'Alcalá, M.,  
717 Vaqué, D., and Zingone, a.: Plankton in the open Mediterranean Sea: a review,  
718 *Biogeosciences*, 7, 1543–1586, <https://doi.org/10.5194/bg-7-1543-2010>, 2010.
- 719 Sisma-Ventura, G., Belkin, N., Rubin-Blum, M., Jacobson, Y., Hauzer, H., Bar-Zeev, E., and  
720 Rahav, E.: Discharge of polyphosphonate-based antiscalants via desalination brine: impact on  
721 seabed nutrient flux and microbial activity, *Environ. Sci. Technol.*,  
722 <https://doi.org/10.1021/acs.est.2c04652>, 2022.
- 723 Sommer, U.: Maximal growth rates of Antarctic phytoplankton: Only weak dependence on  
724 cell size, *Limnol. Oceanogr.*, 34, 1109–1112, <https://doi.org/10.4319/lo.1989.34.6.1109>,  
725 1989.
- 726 Stawiarski, B., Buitenhuis, E. T., and Quéré, C. Le: The physiological response of  
727 picophytoplankton to temperature and its model representation, *Front. Mar. Sci.*, 3, 1–13,  
728 <https://doi.org/10.3389/fmars.2016.00164>, 2016.
- 729 To, S. W., Acevedo-Trejos, E., Chakraborty, S., Pomati, F., and Merico, A.: Grazing  
730 strategies determine the size composition of phytoplankton in eutrophic lakes, *Limnol.*  
731 *Oceanogr.*, 69, 933–946, <https://doi.org/10.1002/lno.12538>, 2024.
- 732 Ungerer, J., Wendt, K. E., Hendry, J. I., Maranas, C. D., and Pakrasi, H. B.: Comparative  
733 genomics reveals the molecular determinants of rapid growth of the cyanobacterium  
734 *Synechococcus elongatus* UTEX 2973, *Proc. Natl. Acad. Sci.*, 115, E11761–E11770,  
735 <https://doi.org/10.1073/pnas.1814912115>, 2018.
- 736 Vaultot, D., Eikrem, W., and Viprey, M.: The diversity of small eukaryotic phytoplankton (3  
737  $\mu\text{m}$ ) in marine ecosystems, *FEMS Microbiol. Ecol.*, 32, 795–820,  
738 <https://doi.org/10.1111/j.1574-6976.2008.00121.x>, 2008.
- 739 Verdy, A., Follows, M., and Flierl, G.: Optimal phytoplankton cell size in an allometric  
740 model, *Mar. Ecol. Prog. Ser.*, 379, 1–12, <https://doi.org/10.3354/meps07909>, 2009.
- 741 Wang, F., Wei, Y., Zhang, G., Zhang, L., and Sun, J.: Picophytoplankton in the West Pacific  
742 Ocean: A Snapshot, *Front. Microbiol.*, 13, 811227,  
743 <https://doi.org/10.3389/fmicb.2022.811227>, 2022.
- 744 Ward, B. A., Marañón, E., Sauterey, B., Rault, J., and Claessen, D.: The size dependence of



745 phytoplankton growth rates: A trade-off between nutrient uptake and metabolism, *Am. Nat.*,  
746 189, 170–177, <https://doi.org/10.1086/689992>, 2017.

747 Welschmeyer, N. A.: Fluorometric analysis of chlorophyll a in the presence of chlorophyll b  
748 and pheopigments, *Limnol. Oceanogr.*, 39, 1985–1992, 1994.

749 Winter, J., Hynes, A., Berthiaume, C., Cain, K., Armbrust, E. V., and Ribalet, F.: Shifts in  
750 phytoplankton community structure across oceanic boundaries, *PLoS One*, 20, 1–16,  
751 <https://doi.org/10.1371/journal.pone.0324466>, 2025.

752 Yacobi, Y. Z. Y., Zohary, T., Kress, N., Hecht, A., Robarts, R. D., Waiser, M., Wood, A. M.,  
753 and Li, W. K. W.: Chlorophyll distribution throughout the southeastern Mediterranean in  
754 relation to the physical structure of the water mass, *J. Mar. Syst.*, 6, 179–190,  
755 [https://doi.org/10.1016/0924-7963\(94\)00028-A](https://doi.org/10.1016/0924-7963(94)00028-A), 1995.

756 Yogeve, T., Rahav, E., Bar-Zeev, E., Man-Aharonovich, D., Stambler, N., Kress, N., Béjà, O.,  
757 Mulholland, M. R., Herut, B., and Berman-Frank, I.: Is dinitrogen fixation significant in the  
758 Levantine Basin, East Mediterranean Sea?, *Environ. Microbiol.*, 13, 854–871, 2011.

759 Zubkov, M. V., Tarran, G. A., and Fuchs, B. M.: Depth related amino acid uptake by  
760 *Prochlorococcus* cyanobacteria in the Southern Atlantic tropical gyre, *FEMS Microbiol.*  
761 *Ecol.*, 50, 153–161, <https://doi.org/https://doi.org/10.1016/j.femsec.2004.06.009>, 2004.

762